Fatal dysfunction and disintegration of thrombin-stimulated platelets

Oleg V. Kim,[1,2] Tatiana A. Nevzorova,[3] Elmira R. Mordakhanova,[3] Anastasia A. Ponomareva,[3,4] Izabella A. Andrianova,[3] Giang Le Minh,[3] Amina G. Daminova,[3,4] Alina D. Peshkova,[3] Mark S. Alber,[2] Olga Vagin,[5,6] Rustem I. Litvinov[1,3] and John W. Weisel[1]

[1]University of Pennsylvania Perelman School of Medicine, Department of Cell and Developmental Biology, Philadelphia, PA, USA; [2]University of California Riverside, Department of Mathematics, Riverside, CA, USA; [3]Kazan Federal University, Institute of Fundamental Medicine and Biology, Kazan, Russian Federation; [4]Kazan Institute of Biochemistry and Biophysics, FRC Kazan Scientific Center of RAS, Kazan, Russian Federation; [5]Geffen School of Medicine at UCLA, Department of Physiology, Los Angeles, CA, USA and [6]VA Greater Los Angeles Healthcare System, Los Angeles, CA, USA

 doi:10.3324/haematol.2018.202309

Received: July 18, 2018.

Accepted: February 14, 2019.

Pre-published: February 21, 2019.

Correspondence: *JOHN WEISEL* - weisel@pennmedicine.upenn.edu

Supplemental Information

Fatal dysfunction and disintegration of thrombin-stimulated platelets

Running title: *Dysfunction and Disintegration of Platelets*

Oleg V. Kim[1,2], Tatiana A. Nevzorova[3], Elmira R. Mordakhanova[3], Anastasia A. Ponomareva[3,4], Izabella A. Andrianova[3], Giang Le Minh[3], Amina G. Daminova[3,4], Alina D. Peshkova[3], Mark S. Alber[2], Olga Vagin[5,6], Rustem I. Litvinov[1,3], and John W. Weisel[1]

[1]University of Pennsylvania Perelman School of Medicine, Department of Cell and Developmental Biology, Philadelphia, Pennsylvania 19104, USA
[2]University of California Riverside, Department of Mathematics, Riverside, California 92505, USA
[3]Kazan Federal University, Institute of Fundamental Medicine and Biology, Kazan 420012, Russian Federation
[4]Kazan Institute of Biochemistry and Biophysics of the Russian Academy of Sciences, Kazan 420111, Russian Federation
[5]Geffen School of Medicine at UCLA, Department of Physiology, CA, 90073, USA
[6]VA Greater Los Angeles Healthcare System, Los Angeles, CA, 90073, USA

Supplemental Figures

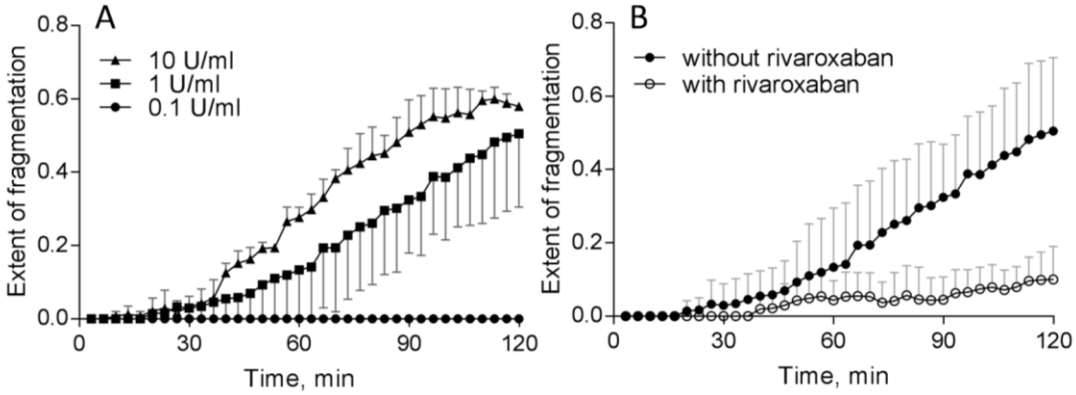

Figure S1. Impact of the thrombin concentration on the extent of platelet fragmentation. The time course of platelet fragmentation in PRP clots at 0.1, 1.0, and 10 U/ml thrombin concentrations (**A**) and 1 U/ml thrombin-induced platelet fragmentation in the presence and absence of rivaroxaban (**B**) in re-calcified PRP clots (M±SD, n=50-100 cells analyzed for a clot from 3 donors for each experimental condition).

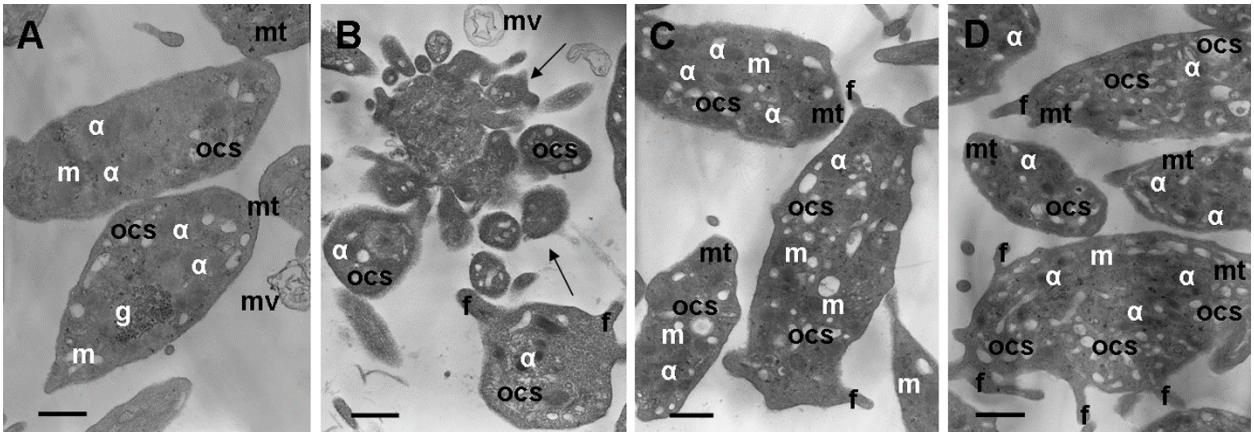

Figure S2. Impact of various stimuli on platelet integrity. Representative transmission electron micrographs of isolated control untreated platelets (**A**), a fragmented platelet (arrow) treated with 1 U/ml thrombin (**B**) in contrast to non-fragmented platelets treated with either 5 µM ADP (**C**) or 5 µg/ml soluble collagen (**D**). All the samples were incubated for 2 hours at 37ºC in Tyrode's buffer with 2 mM Ca^{2+}. The designated structures are α-granules (α), glycogen granules (g), mitochondria (m), microtubules (mt), open canalicular system (ocs), filopodia (f) and microvesicles (mv). Magnification bars = 0.5 µm.

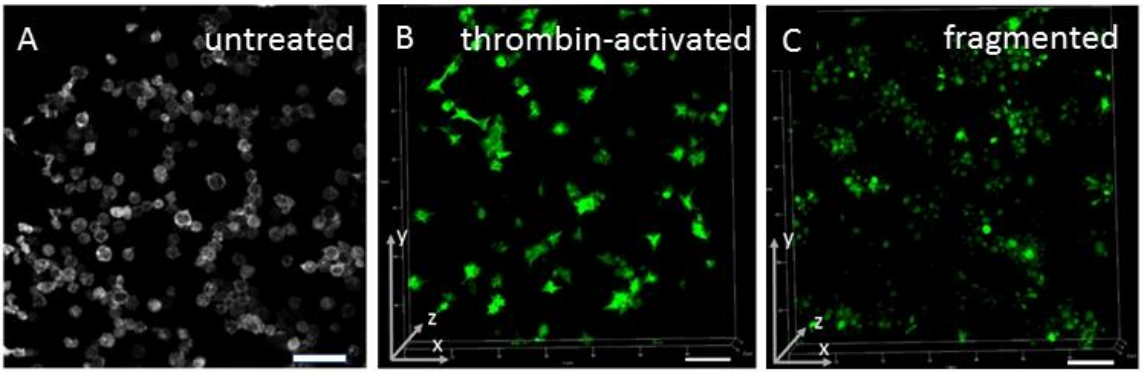

Figure S3. Low magnification images of phalloidin-stained F-actin in control untreated (A) and thrombin-activated platelets before (B) and after (C) fragmentation (3-hr-incubation) detected by fluorescence confocal microscopy. A dramatic increase in the fluorescence intensity of F-actin in platelets after thrombin treatment (see Figure 4 in the main text) was compensated for by a higher amplification gain for the green channel in untreated samples as compared with thrombin-treated samples. Scale bars = 10 μm.

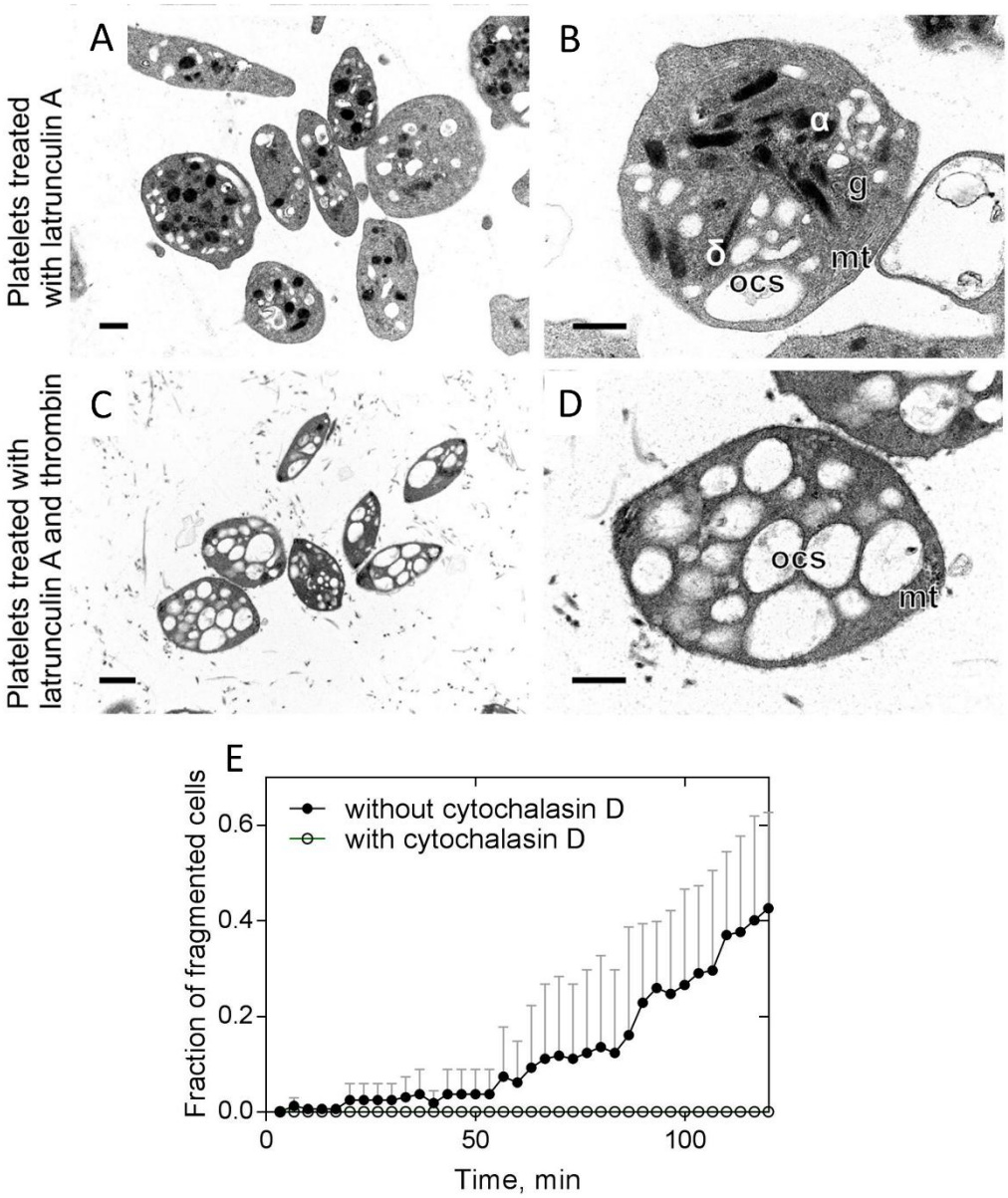

Figure S4. Impact of latrunculin A and cytochalasin D on platelet fragmentation. Representative transmission electron micrographs of isolated platelets incubated with latrunculin A (**A, B**) and latrunculin A combined with 1 U/ml thrombin (**C, D**) for 15 min at 37°C in Tyrode's buffer containing 2 mM $CaCl_2$. No platelet fragmentation was observed in the presence of latrunculin A. The designated structures are α-granules (α), δ-granules (δ), glycogen granules (g), microtubules (mt), open canalicular system (ocs). Scale bars = 0.5 µm. (**E**) Complete prevention of thrombin-induced platelet fragmentation by cytochalasin D (M±SD, 50-100 cells analyzed for each PRP clot from 3 donors).

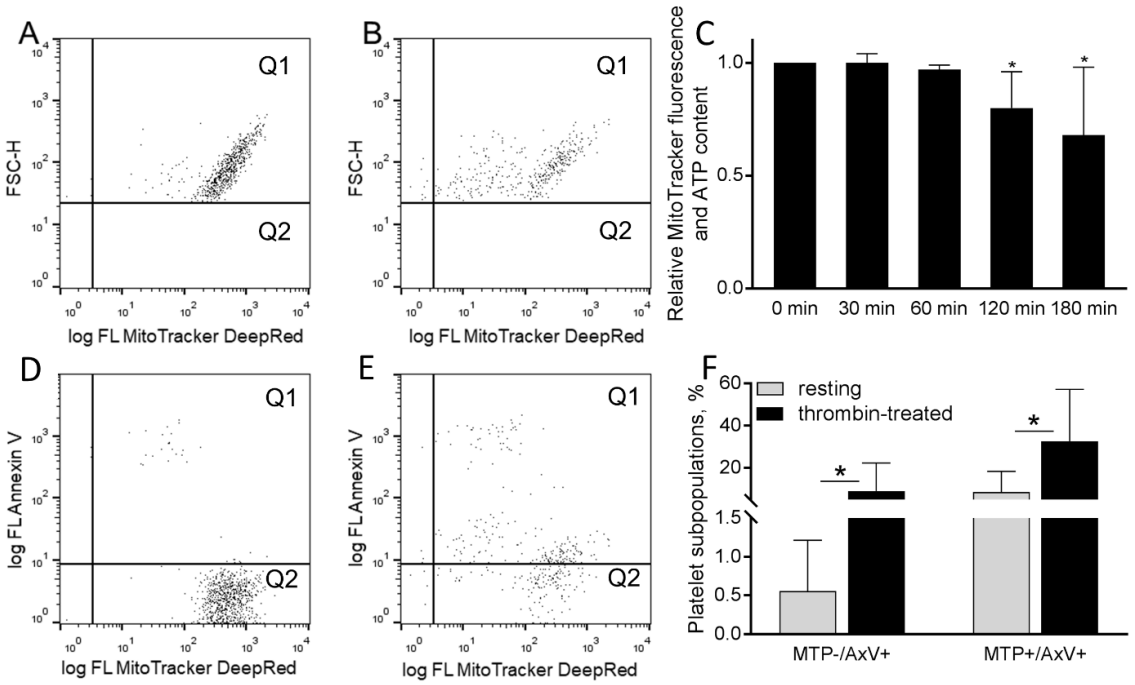

Figure S5. **Flow cytometry-based determination of the mitochondrial transmembrane potential (MTP) and phosphatidylserine expression in isolated platelets.** (**A,B**) Representative dot-plots showing MitoTracker-positive platelets (Q1) detected after incubation of untreated (A) and thrombin-treated (B) platelets in Tyrode's buffer at 37°C for 60 min with 2 mM $CaCl_2$ and presented as log FL MitoTrackerDeepRed vs. FSC dot-plots. (**C**) Time-dependent changes of MTP in platelets activated with 1 U/ml thrombin in Tyrode's buffer with Ca^{2+} at 37°C (*n*=3). The data are normalized by their initial values and the values for untreated platelets at the corresponding time points. (**D,E)** Representative dot-plots showing subpopulations of MitoTracker-positive/Annexin V-positive (quadrant Q1) and MitoTracker-positive/Annexin V-negative (quadrant Q2) platelets after incubation in Tyrode's buffer at 37°C for 15 min for two different conditions: (D) untreated platelets (negative control) and (E) platelets incubated with 1 U/ml thrombin. (**F**) Subpopulations of Annexin V-positive (AxV+) platelets expressing phosphatidylserine with extinct (MTP-) or maintained (MTP+) mitochondrial transmembrane potential after 60 min of incubation with 1 U/ml thrombin in Tyrode's buffer at 37°C with 2 mM Ca^{2+} (n=9).

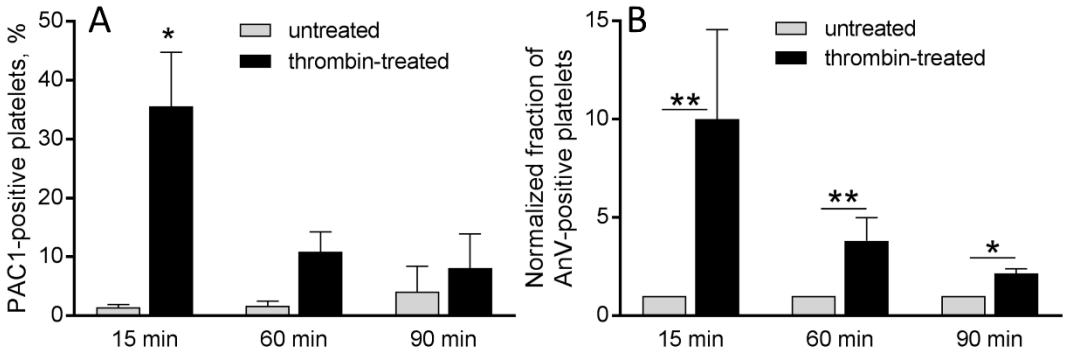

Figure S6. Thrombin-induced integrin αIIbβ3 activation and phosphatidylserine exposure in isolated platelets determined using flow cytometry. (A) Time-dependent changes of the fraction of PAC1-positive (expressing the active αIIbβ3) isolated platelets after incubation without (grey bars) or with 1 U/ml thrombin (black bars) in Tyrode's buffer with Ca^{2+} at 37°C (n=3). **P*<0.05 compared to untreated platelets. The difference between the consecutive measurements at 15 vs 60 min is also significant, *P*<0.05. (B) Fraction of Annexin V-positive (AnV+) isolated platelets expressing phosphatidylserine measured after incubation without (grey bars) or with 1 U/ml thrombin (black bars) in Tyrode's buffer with Ca^{2+} at 37°C (n=4). The data are normalized by the corresponding values for control untreated platelets. **P*<0.05, ***P*<0.01 compared to the untreated platelets. A difference between the consecutive measurements at 15 vs 60 min and 60 vs 90 min is also significant, *P*<0.05. A two-tailed Mann-Whitney *U* test.

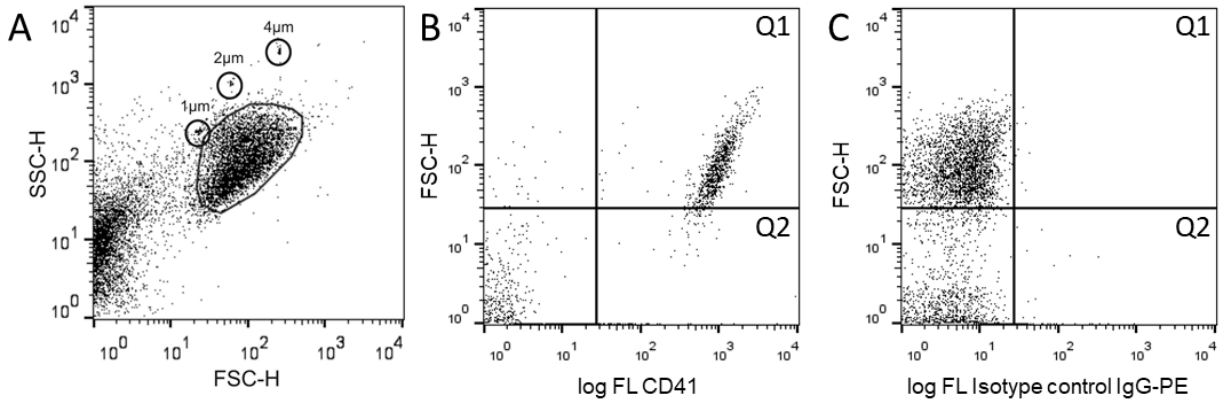

Figure S7. Flow cytometry-based identification of platelets and platelet-derived microparticles. (**A**) Gel-filtered isolated untreated platelets and calibration polystyrene beads (1 μm, 2 μm, and 4 μm in diameter) were suspended in Tyrode's buffer. Platelets are shown in the outlined gate in a two-channel FSC vs. SSC modes (distribution by size and granularity, respectively). (**B**) Untreated isolated platelets (negative control) incubated with PE-conjugated antibodies to CD41 in Tyrode's buffer at 37°C for 15 min analyzed by flow cytometry (log FL CD41 vs. FSC) and detected as CD41-positive platelets (quadrant Q1) and CD41-positive platelet fragments (quadrant Q2). (**C)** Control untreated platelets labeled with isotype control to the anti-CD41-PE-antibodies incubated under the same conditions and analyzed at the same flow cytometry settings as in (**B**). The horizontal borderline between Q1 and Q2 in A-C was determined using a FCS signal for 1-μm calibration polystyrene beads shown in (**A**).

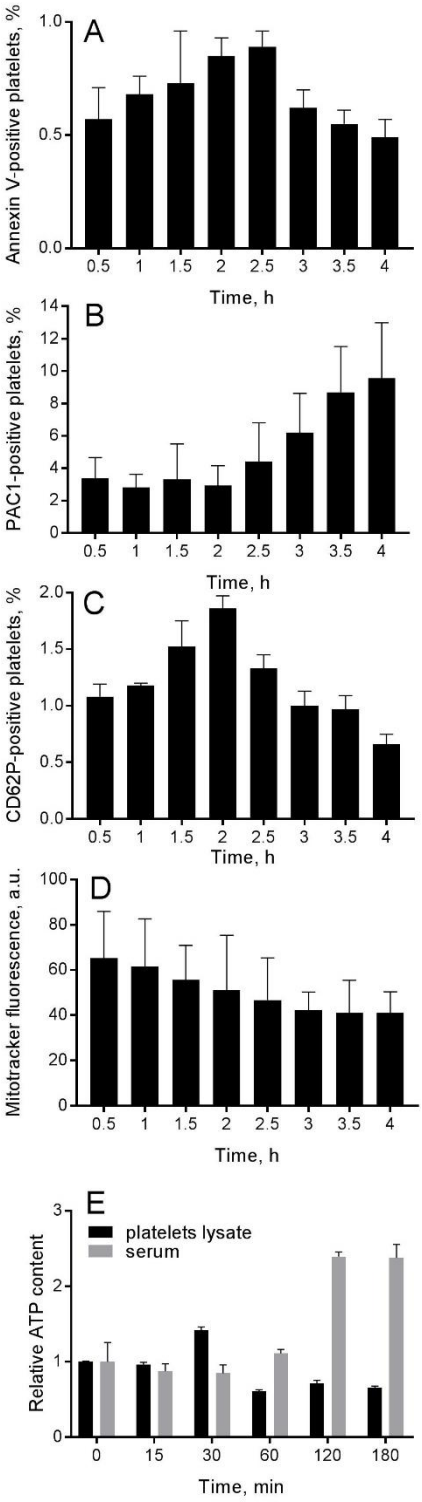

Figure S8. Non-specific changes of molecular markers of platelet activation and dysfunction during storage of control untreated platelets. Spontaneous expression of (**A**) phosphatidylserine, (**B**) active integrin αIIbβ3 determined by PAC-1 binding, (**C**) P-selectin, along with (**D**) mitochondrial transmembrane potential, (**E**) extra- and intracellular ATP content in resting (untreated) platelets in freshly obtained PRP kept at 37ºC for 3(E) hours or 4(A-D) hours (n=3-5).

Supplemental Movies

Supplemental Movie S1. A 60 min time-lapse confocal microscopy-based 3D reconstruction of thrombin-induced fragmentation of single platelets and platelet aggregates (green) in a contracting plasma clot.

Supplemental Movie S2. Confocal microscopy-based 3D reconstruction of widespread fragmentation of thrombin-treated platelets (green) within a PRP clot prepared as in Figure 1A after 3 hours of incubation.

Supplemental Movie S3. A 120 min confocal microscopy-based dynamics of ROS production in fragmented platelets in PRP clots. Mitochondrial ROS is detected by MitoSOX™ Red shown in red; calcein AM-labeled platelets are green.

Supplemental Movie S4. A 120 min confocal microscopy-based dynamics of ROS production in fragmented platelets in PRP clots. Mitochondrial ROS is detected by MitoSOX™ Red shown in red; calcein AM-labeled platelets are green. A magnified variant of the process shown in the Supplementary Movie S3.

Supplemental Methods

Platelet-rich plasma

For experiments with platelet-rich plasma (PRP), blood was drawn by venipuncture from healthy volunteers not taking any medications known to affect platelet function for at least 14 days. Informed consent was obtained in accordance with a protocol approved by the University of Pennsylvania Institutional Review Board and was in compliance with the Helsinki Declaration of ethical principles for medical research involving human subjects. All procedures were carried out in accordance with the approved guidelines. To obtain PRP, whole blood stabilized with 3.2% trisodium citrate (9:1 v/v) was centrifuged at 210g at 25°C for 15 min within 30 min after blood withdrawal. The PRP was kept at room temperature and used within 4 hours after blood collection. Of the total 42 volunteers enrolled in the study, in 15 the platelet count in blood was measured. The platelet counts varied from 180,000/µl to 320,000/µl with an average 276,000±60,000/µl (M±SD).

In a set of inhibitory experiments, PRP samples were pre-incubated for 30 min with 1 μM latrunculin A (Sigma-Aldrich, USA) or 10 μM cytochalasin D (Sigma-Aldrich, USA) to impair actin polymerization, 10 μM paclitaxel (Invitrogen, USA) to inhibit microtubule dynamics, 100 μM blebbistatin (Sigma-Aldrich, USA) to block myosin IIa, 1 μM rivaroxaban (Selleck Chemicals, USA) to inhibit factor Xa and prevent generation of endogenous thrombin, or 100 μM ALLN (Calbiochem, USA) to suppress calpain activity.

Activation of platelets by thrombin and formation of PRP-clots for confocal microscopy

Clotting of citrated PRP and platelet activation were induced by adding human thrombin (Sigma-Aldrich, cat. # T4393, 1 U/ml final concentration unless otherwise indicated) and $CaCl_2$ (26 or 31 mM final concentration, which is equivalent to ~1 mM or ~6 mM free Ca^{2+}, respectively). Immediately after activation, 30-µl PRP samples were quickly transferred onto 35 mm x 10 mm PELCO® clear wall glass bottom cell culture dishes in the environmental chamber of the confocal microscope for real-time dynamic imaging of fluorescently labeled platelets and other clot components.

Labeling of platelets and other components of PRP-clots to visualize with fluorescent confocal microscopy

Various fluorescent probes were added to PRP before activation with thrombin to visualize clot components in a confocal microscope. Live platelets were labeled with calcein AM (Molecular Probes, 0.2 µg/ml final concentration); the intracellular [Ca^{2+}] dynamics was imaged using a Ca^{2+}-dependent fluorophore Fluo-4AM (Invitrogen, USA); fibrin was visualized by adding Alexa Fluor 647- or Alexa Fluor 594-labeled human fibrinogen (Molecular Probes, Grand Island, NY, 40 µg/ml final concentration); metabolically active mitochondria were labeled with $\Delta\psi_m$-sensitive fluorescent dye MitoTracker Red FM (Invitrogen, Oregon, USA, 1 µM final concentration) or 200 nM tetramethylrhodamine, methyl ester, perchlorate (Invitrogen, USA). To quantify reactive oxygen species (ROS), platelets in PRP were loaded with 5 μM of MitoSOX™ Red (Invitrogen, USA) and pre-incubated for 20 min at 37°C in the dark before adding

thrombin. To track ATP production in live platelets, PRP was pre-incubated with BioTracker ATP-Red Live Cell Dye (Millipore-Sigma, USA) for 20 min at 37ºC. In a set of experiments, PRP was pre-incubated with CellEvent™ Caspase-3/7 Green Detection Reagent (C10427, Invitrogen, 20 µM final concentration) to track the caspase 3 and 7 activity. The fluorescent probes were added to PRP and incubated for 20 min at 37ºC before initiation of clotting of the plasma samples with 1 U/ml thrombin and 31 mM $CaCl_2$. To evaluate the activity of intracellular calpain, PRP samples were pre-incubated at 37°C for 30 min with 100 µM Calpain Substrate IV (Calbiochem, USA), a cell-penetrating substrate containing Dabcyl and EDANS fluorophores, followed by incubation with 1 U/ml human thrombin (Sigma-Aldrich, USA) for up to 90 minutes. PRP samples incubated with 100 µM calcium ionophore A23187 (Sigma Aldrich, USA) were used as a positive control for calpain and caspase activities and untreated PRP samples were used as a negative control.

Confocal microscopy of fluorescently labeled PRP clots

Clots freshly formed on a microscope cover glass were imaged in a Zeiss LSM810 laser confocal microscope with Plan Apo 40x (NA 1.2) water immersion objective lens to obtain a series of high-resolution 212.5 µm x 212.5 µm x 20 µm z-stack images taken each 5 min during 60-90 min after clot formation. The distance between each z-stack slice was 0.6 µm with a resolution of 1024x1024 pixels; voxel size was 0.2076 x 0.2076 x 0.6896 μm^3. A combination of an argon laser beam with a 488-nm wavelength and a helium-neon laser with a 633-nm wavelength was utilized to visualize calcein AM- or Fluo4 AM-labeled platelets and fibrin. To detect activation of caspase 3/7 in platelets and changes in the transmembrane potential of platelet mitochondria, an argon laser beam with a 488-nm wavelength was used in combination with a Diode-Pumped Solid-State laser with 561-nm wavelength to track fluorescence of caspase-3/7 fluorogenic substrate (green) and platelet mitochondria (red), respectively. An argon laser beam with a 405-nm excitation wavelength was used to detect EDANS fluorescence resulting from cleavage of Calpain Substrate IV as a measure of calpain activity. ATP fluorescence in live platelets was detected by using a 488-nm argon laser beam. To follow mitochondrial ROS production, a 561-nm argon laser beam was applied for excitation of the mitochondrial superoxide indicator.

Measurements of ATP content in platelets in PRP clots

We have applied a BioTracker ATP-Red (Millipore-Sigma, USA) live cell dye to assess temporal alterations of intracellular ATP content in platelets in PRP-clots. PRP samples were pre-incubated with the dye for 20 minutes followed by addition of thrombin and collection of high-resolution confocal z-stack images to visualize temporal changes in fluorescence of the BioTracker. Quantification of changes in the level of ATP was as follows. First, for each consequent time point, a sum z-stack projection was calculated and the integrated fluorescence intensity, I_T, was measured using a standard function in ImageJ. Next, the background fluorescence was measured and subtracted from I_T to get the fluoresce intensity of platelets of the imaged volume. Finally, platelet fluorescence intensity at each time point, *t*, divided by the total number of platelets in the volume was

normalized by its initial value, $I = I_T(t)/I_T(0)$, thus providing relative changes in the fluorescence of the imaging probe corresponding to changes of platelet ATP.

Measurements of mechanical stress in contracting PRP clots

To measure the dynamic contractile force induced by fibrin-attached activated platelets, a rheometer (ARG2; TA Instruments, New Castle, DE, USA) was used. Clots were formed in a 400-μm gap between a 20-mm flat parallel top plate and a fixed bottom plate of the rheometer by adding 1 U/ml thrombin and 31 mM $CaCl_2$ to PRP. The contractile force was measured as a negative normal (vertical) force applied to the horizontal rheometer plates by the contracting clot. To prevent sample dehydration at the clot-air interface, a thin layer of silicone oil was applied at the clot edge.

Isolation and enumeration of platelets

Platelets were isolated from the blood of healthy volunteers not taking any medications known to affect platelet function for at least 14 days. Blood samples were collected following informed consent under approval of the Ethical Committee of the Interregional Clinical and Diagnostic Center (Kazan, Russian Federation). All procedures were carried out in accordance with the approved guidelines. Blood was drawn via venipuncture into 3.8% trisodium citrate (9:1 v/v). Immediately after collection, citrated blood was centrifuged at room temperature at 200g for 10 min to obtain PRP. Platelets were isolated from PRP by gel-filtration on Sepharose 2B (GE Healthcare, Sweden) equilibrated with Tyrode's buffer (4 mM HEPES, 135 mM NaCl, 2.7 mM KCl, 2.4 mM $MgCl_2$, 5.6 mM D-glucose, 3.3 mM NaH_2PO_4, 0.35 mg/ml bovine serum albumin, pH 7.4). Platelet count was performed in a hemocytometer with a 400x magnification. Isolated platelets were used within 3 hours after blood collection.

Transmission electron microscopy of isolated platelets and platelet fragments

Freshly isolated gel-filtered platelets in Tyrode's buffer were activated by adding 1 U/ml human thrombin (Sigma-Aldrich), 5 μg/ml collagen (Type I from calf skin, water soluble, RENAM, Russia) or 5 μM adenosine diphosphate (Chrono-log, USA) in the presence of 2 mM $CaCl_2$ followed by incubation at 37°C for 15 min, 60 min or 2 hours. Untreated platelets incubated at 37°C were used as a negative control. The final volume of each sample was 560 μl containing about $80x10^6$ platelets/ml. Immediately after incubation, the platelet suspension was fixed by adding 2.5% glutaraldehyde (final concentration) for 30 min at room temperature and then centrifuged at 1,000g for 5 min. The precipitate was washed with Tyrode's buffer and then postfixed with 1% osmium tetroxide in the same buffer supplemented with sucrose (25 mg/ml) for 2 hours. The samples were dehydrated in ascending ethanol concentrations, acetone, and propylene oxide. The Epoxy resin medium was Epon 812 (Fluka, Switzerland). The samples were allowed to polymerize for 3 days at an increasing temperature from 37°C to 60°C. Ultrathin sections were cut using an LKB ultramicrotome-III (LKB, Sweden) and stained with saturated aqueous uranyl acetate (Serva, Germany) at 60°C for 10 minutes and lead citrate (Serva, Germany) at room temperature for 10 minutes. The specimens were examined using a JEM-1200EX

electron microscope (JEOL, Japan) at an operating voltage of 80 kV. The ultrastructure of cells at each experimental condition studied was studied in three independent platelet preparations with at least three samples processed from each cell preparation. Not less than 40-50 ultrathin sections were viewed and analyzed followed by imaging of at least 150-200 cells at each experimental condition.

Scanning electron microscopy of isolated platelets

After incubation with (1 U/ml) or without thrombin in the presence of 2 mM $CaCl_2$, isolated platelets (10^6 cells in 150 µL) were fixed with 4% glutaraldehyde solution (1:1 v/v) in 50 mM cacodylate buffer, pH 7.4, containing 150 mM NaCl, or in PBS for 60 min at room temperature. Fixed platelets (300 µL) were layered on a carbon filter with 0.4-µm or 0.1-µm pore size (EMD Millipore) and centrifuged at 150g for 15 min. Samples were washed three times in the cacodylate buffer or PBS, dehydrated in ascending ethanol concentrations and dried overnight with hexamethyldisilazane (Electron Microscopy Sciences). Gold-palladium (~15 nm) was layered on the samples using a sputter coater (Polaron e5100, Quorum Technologies, UK or Quorum Q 150T ES, UK). Scanning electron micrographs were taken at 5-10kV using Quanta FEG 250 (FEI, USA) or Merlin (Carl Zeiss, Germany) microscopes.

Flow cytometry of untreated platelets in PRP

Citrated PRP was kept at 37ºC, 3-µl-aliquots were taken out every 30 min, mixed with 47 µl of Tyrode's buffer and platelets were labeled with one of the following reagents: Annexin V conjugated with FITC (BioLegend, USA), anti-human-CD62p antibodies conjugated with PE (BD Biosciences, USA), FITC-conjugated PAC-1 antibodies against activated αIIbβ3 (BD Biosciences, USA), a $\Delta\Psi_m$-sensitive fluorescent dye MitoTracker DeepRed FM (Invitrogen, USA). Labeled platelets were added to the Ca^{2+}-containing buffer (10 mM HEPES, 140 mM NaCl, 2 mM $CaCl_2$, pH 7.4) followed by flow cytometry. The measurements were performed up to 4 hours during storage of freshly obtained PRP.

Flow cytometry of isolated platelets and platelet-derived microparticles

Freshly isolated 200,000 platelets in 150 µl Tyrode's buffer were incubated at 37°C up to 90 min without (negative control) or with 1 U/ml thrombin. During flow cytometry, platelets were identified in the dot plots based on their size and granularity using forward light scatter (FSC) and side light scatter (SSC) channels and gated after size-based calibration with 1-µm-, 2-µm-, and 4-µm-polystyrene beads (ThermoFisher, USA) **(Figure S7A)**. The size-based platelet gate was confirmed by the ability of platelets to bind anti-CD41-PE-labeled antibodies (Invitrogen, USA) (the size-based platelet gate contained ~98% of CD41-positive events, data not shown). Platelet-derived microparticles were identified and quantified as the events that reflected a platelet-specific marker CD41 (platelet integrin's subunit αIIb) and were characterized by forward light scatter (FSC) smaller than 1 µm using FSC/FL CD41 (FL CD41 is a flow cytometry channel for phycoerythrin fluorescence) dot plots (**Figure S7B,C**). 30,000 events were collected using a FacsCalibur flow cytometer (BD Biosciences, USA) for each measurement.

To reveal changes in the mitochondrial transmembrane potential ($\Delta\psi_m$), platelets were labeled by a $\Delta\psi_m$-sensitive fluorescent dye MitoTracker DeepRed FM (150 nM final concentration) (Invitrogen, USA). Depolarization of the mitochondrial membrane was characterized by the reduction in the mean fluorescence intensity of platelet-bound MitoTracker (**Figure S5)**. To assess expression of the phosphatidylserine on the plasma membrane of platelets and/or platelet-derived microparticles, thrombin-treated isolated platelets were centrifuged at 1,000g for 5 min and re-suspended in 150 µl of a Ca^{2+}-containing buffer (10 mM HEPES, 140 mM NaCl, 2 mM $CaCl_2$, pH 7.4). The pellet was treated for 10 min at room temperature in the dark with FITC-labeled Annexin V (BioLegend, USA) and with anti-CD41 PE-conjugated antibodies (Invitrogen, USA) followed by flow cytometry. Platelets gated using FSC and SSC that expressed phosphatidylserine and exhibited fluorescence of platelet-bound MitoTracker were quantified in four dot-plot quadrants using CellQuest Pro (BD Biosciences, USA) and FlowJo software. Unlabeled platelets and platelet microparticles were used as controls to the fluorescing particles gated in the corresponding dot plots (**Figure S7**). At least four independently isolated platelet preparations were examined under each experimental condition.

To evaluate the activity of caspase 3 and 7 in platelets stimulated by thrombin (1 U/ml) or calcium ionophore A23187 (10 µM) used as a positive control, platelets were incubated with CellEvent™ Caspase-3/7 Green Detection Reagent (C10427, ThermoFisher, 500 nM final concentration) for 30 min following 60 min of incubation with thrombin or A23187 in the presence of 2 mM $CaCl_2$ and analyzed using flow cytometry. Platelet caspase activity was characterized in terms of fluorescence intensity in arbitrary units of the fluorogenic substrate for caspases 3 and 7 in the FL1 channel. A total of 30,000 events were collected for each sample.

Measurement of ATP content in platelets and extracellular liquid

Isolated gel-filtered platelets (0.1 ml at 10^7 cells/ml) in Tyrode's buffer were incubated for various time intervals without or with 1 U/ml human thrombin in the presence of 2 mM $CaCl_2$. After the incubation, platelets were spun down for 5 min at 2,000g and lysed with 0.2% Triton X-100 in Tyrode's buffer for 20 min at room temperature with continuous shaking. Debris was removed from the lysates by centrifugation at 8,000g for 10 min. ATP concentration in the platelet lysates was measured with a plate reader, Infinite 200 PRO (Tecan, Switzerland) using an ATP Bioluminescent Assay Kit (Sigma-Aldrich) according to the manufacturer's instructions.

To evaluate long-term effects of thrombin on the intra- and extracellular ATP content, citrated human PRP was diluted with Tyrode's buffer containing 2 mM $CaCl_2$ to a final concentration of platelets 10^7/ml (~50-fold). 1 U/ml thrombin (final) was added to 6 PRP samples (0.1 ml each) that were analyzed sequentially at various time points. Before and after 15, 30, 60, 90, 120, and 180 min of incubation with thrombin each sample (all clotted except the one without thrombin) was spun down at 2,000g for 5 min. The platelet pellet

was lysed and processed for the ATP measurement as described above in parallel with the activated platelet supernatant following clot formation.

To determine if platelet ATP content changes during storage in the absence of thrombin, citrated human PRP was supplemented with 26 mM $CaCl_2$ in the presence of 2 U/ml hirudin (both final concentrations), which was added to suppress potential thrombin activity. Aliquots (0.1 ml) of PRP were taken every 30 min and platelets were spun down followed by their lysis and ATP measurement as described above.

Fluorimetric measurement of calpain activity in isolated platelets

Gel-filtered human platelets (200,000 in 150 µl Tyrode's buffer containing 2 mM $CaCl_2$) were incubated with 10 µM Calpain Substrate IV (Calbiochem, USA) at 37° C for 3 hours followed by incubation for 15, 60, and 180 minutes at 37°C with 1 U/ml and 5 U/ml human thrombin (Sigma-Aldrich, USA). The EDANS fluorescence intensity was measured at 380±20 nm excitation and 465±30 nm emission wavelengths on a multimode plate reader Infinite F Plex (Tecan, Switzerland). Platelets incubated with 100 µM calcium ionophore A23187 (Sigma Aldrich, USA) were used as a positive control and untreated platelets were used as a negative control.

Western blot analysis of procaspase 3 cleavage

Isolated platelets, untreated (negative control) or treated with either 1 U/ml thrombin or 10 µM calcium ionophore A23187 (positive control), were supplemented with a lysis RIPA buffer (pH 7.4) containing a proteinase inhibitor cocktail, and the mixture was incubated at 4ºC overnight with continuous shaking. The samples were centrifuged at 8,000g for 10 min at 4ºC and the supernatants were collected. Cell lysates were suspended in a sodium dodecyl sulfate (SDS) sample-loading buffer, boiled for 3 min and subjected to gradient 12-20% SDS-PAGE. After protein transfer the nitrocellulose membranes with a 0.2 µm pore size (BioRad, USA) were incubated overnight at 4°C with antibodies against human (pro)caspase 3 (Millipore Sigma, USA, cat. # MAB4703, clone 4-1-18). To detect the primary antibodies, blots were incubated with the secondary goat horseradish peroxidase-conjugated anti-mouse IgG antibodies (Invitrogen, USA). Blots were analyzed using a ChemiDoc Xrs+ System (BioRad, USA).

Image analysis

The images of platelets obtained with confocal and scanning electron microscopy were analyzed using the open source Fiji software to characterize platelet fragmentation and changes in the fluorescence intensities of the MitoTracker $\Delta\psi_m$-sensitive fluorescent dye and fluorogenic substrate for caspase 3/7. Visualization and maximum intensity projection of z-stacks of platelet-fibrin 3D meshworks were done in Fiji. Numerical and graphical data analysis and presentation were done in GraphPad Prism 7. Confocal microscopy-based 3D reconstruction of platelets and platelet fragments stained for F-actin or with calcein AM was performed with Imaris software (Imaris, Bitplane, USA) using 10- to 30-µm-thick z-stacks with 0.1 µm distance between z-stack planes.

Statistical analyses
Statistical analyses were performed using a GraphPad Prism 7 package. Statistical significance of the differences inside and between groups of samples were determined by a Mann-Whitney U test with a 95% confidence level. Correlation analysis was based on calculating Spearman's rank coefficient. Results are presented as mean ± standard deviation unless otherwise indicated.

Supplemental results

Specific versus non-specific changes of molecular markers of platelet activation and dysfunction
Flow cytometry not only confirmed a dramatic decrease in the fraction of platelets with retained mitochondrial membrane potential after stimulation with thrombin (**Figure S5A-C**), but it also demonstrated enhanced phosphatidylserine exposure in thrombin-activated platelets, either with or without mitochondrial depolarization (**Figures S5D-F**). This finding suggests the existence of two subpopulations of thrombin-stimulated platelets, namely metabolically active procoagulant platelets (with retained $\Delta\Psi_m$ and exposed phosphatidylserine) and procoagulant but dysfunctional or "dying" platelets (with extinct $\Delta\Psi_m$ and exposed phosphatidylserine) perhaps via a cell death pathway (**Figure S5F**).
Notably, in response to thrombin platelets initially exposed the activated integrin αIIbβ3 (determined by PAC1 binding) followed by a dramatic decrease of PAC1-reactive αIIbβ3 on the surface starting at the time of fragmentation (~30 min) and lasting up to 1.5 hours of observation (**Figure S6A**), which was synchronized with the phosphatidylserine exposure, characterized by the initial increase of the fraction of Annexin-V-positive platelets followed by its significant decrease starting at the onset of fragmentation (**Figure S6B**).

To confirm that expression of the molecular makers and the observed metabolic changes are specific for platelet activation and do not result from non-specific "storage lesion", we followed spontaneous alterations of untreated resting platelets kept at 37ºC in PRP up to 4 hours. The results summarized in **Figure S8** clearly show that the unprovoked time-dependent expression of phosphatidylserine, surface-attached P-selectin and active αIIbβ3, as well as mitochondrial depolarization and a reduction in ATP content all have a much smaller extent and a totally different gradual time course than those observed in thrombin-activated platelets. Therefore, the kinetics of this spontaneous platelet activation/dying is dramatically different from the platelet stimulation followed by deep dysfunction and disintegration observed as a results of thrombin treatment.